



Research Article

Dimensional crossovers in the Gaussian critical fluctuations above T_c of two-layer and three-layer superconductors

A. S. Viz¹ · M. M. Botana¹ · J. C. Verde¹ · M. V. Ramallo^{1,2} 

Received: 27 December 2021 / Accepted: 25 April 2022

Published online: 16 May 2022

© The Author(s) 2022 [OPEN](#)

Abstract

By using a Ginzburg–Landau functional in the Gaussian approximation, we calculate the energy of superconducting fluctuations above the transition, at zero external magnetic field, of a system composed by a small number N of parallel two-dimensional superconducting planes, each of them Josephson coupled to its first neighbour, with special focus in the $N = 2$ and 3 cases. This allows us to obtain expressions for the critical contributions to various observables (fluctuation specific heat and magnetic susceptibility and Aslamazov–Larkin paraconductivity). Our results suggest that these systems may display deviations from pure 2D behaviour and interesting crossover effects, with both similitudes and differences to those known to occur in infinite-layers superconductors. Some challenges for future related research are also outlined.

Article Highlights

- We study superconductors composed of a few parallel layers, in the Gaussian–Ginzburg–Landau approach above their critical temperature.
- We calculate the heat capacity, susceptibility and conductivity induced by critical thermal fluctuations, mainly for bi- and tri-layers.
- We obtain dimensional crossovers in the critical behaviors and compare them with the ones in infinite-layers superconductors.

Keywords Superconductivity in nanosystems · Critical phenomena in superconductors · Twodimensional materials · Lawrence–Doniach models

1 Introduction

The different interplays between reduced dimensionality and superconducting properties is a research subject of increasing activity, fostered by the novel possibilities for fabricating nanosized and/or nanostructured

superconductors [1–4]. Also by the fact that both Cu- and Fe-based high-temperature superconductors are layered materials that may be modelled as stacks of parallel 2D layers [5, 6]. One of the notable effects of low dimensionality is the enhancement of the critical fluctuations near the superconducting transition temperature T_c [6, 7]. For instance, it is well known that in 2D films the

Supplementary Information The online version contains supplementary material available at <https://doi.org/10.1007/s42452-022-05050-8>.

✉ M. V. Ramallo, mv.ramallo@usc.es; ramallo@cond-mat.eu; A. S. Viz, viz@cond-mat.eu; M. M. Botana, botana@cond-mat.eu; J. C. Verde, verde@cond-mat.eu | ¹Quantum Materials and Photonics Research Group (QMatterPhotonics), Department of Particle Physics, University of Santiago de Compostela, 15782 Santiago de Compostela, Spain. ²Instituto de Materiais (iMATUS), University of Santiago de Compostela, 15782 Santiago de Compostela, Spain.



SN Applied Sciences

(2022) 4:175

| <https://doi.org/10.1007/s42452-022-05050-8>

SN Applied Sciences
A SPRINGER NATURE journal

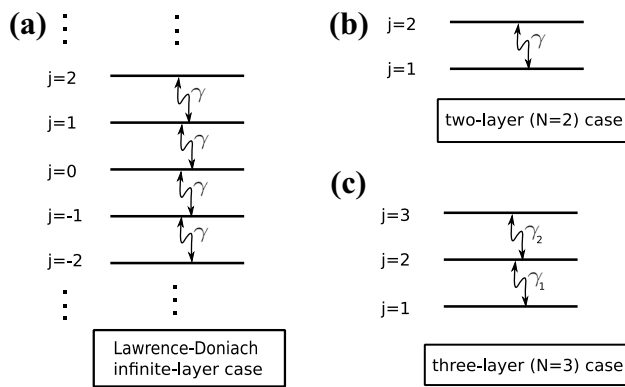


Fig. 1 Panel **a** Schematic representation of a Lawrence–Doniach (LD) or infinite-layer ($N \rightarrow \infty$) superconductor, with single inter-layer distances and Josephson couplings between adjacent layers. Panel **b** Schematic representation of a two-layer superconductor ($N = 2$, see Sects. 2.2 and 4). Panel **c** Schematic representation of a three-layer superconductor ($N = 3$; see Sect. 2.3, and also Sect. 5 for the $\gamma_1 = \gamma_2$ case or Sect. 6 for $\gamma_1 > \gamma_2$). In (**b**, **c**), each layer j may have a different T_{c_j} or a common one; our discussions in Sect.s 4–6 focus in the latter case

superconducting fluctuation-induced contributions to various experimental observables above but near T_c are well larger than in 3D bulks. Not only the amplitude, but also the critical exponent is affected [6, 7]. For instance, in low- T_c superconductors the fluctuation contribution above T_c to the heat capacity, c_{fl} , has in 3D bulks critical exponent $x = 1/2$ [i.e., $c_{fl} \propto \varepsilon^{-1/2}$ with $\varepsilon = \ln(T/T_c)$] and in most cases unobservable amplitude [6, 7], while in 2D films the amplitude is well measurable and the critical exponent is $x = 1$ [6, 7]. (For $T < T_c$, fluctuations are also observable in 2D but display the more complex vortex-antivortex phenomenology famously predicted by Kosterlitz and Thouless [8, 9]). Reduced dimensionality also changes the fluctuation contributions to other observables such as magnetic susceptibility, electrical conductivity, etc. [6].

Some of the richer phenomenologies for the interrelations between low dimensionality and critical fluctuations are provided by layered superconductors. These may be modelled using the Lawrence–Doniach (LD) functional [10], i.e., the Ginzburg–Landau (GL) free energy for a superconductor composed of an infinite (macroscopic) number of parallel planes, each of them Josephson-coupled with its adjacent neighbour. Panel (a) of Fig. 1 schematizes such superconductors. By introducing small (Gaussian) excitations, it is possible to calculate expressions for the critical fluctuations above T_c [10] that are in good agreement with measurements in various macroscopic layered materials, including for instance the Cu- and Fe-based high- T_c superconductors [11–13]. The basic prediction of this LD modelization for the fluctuation-induced heat capacity above

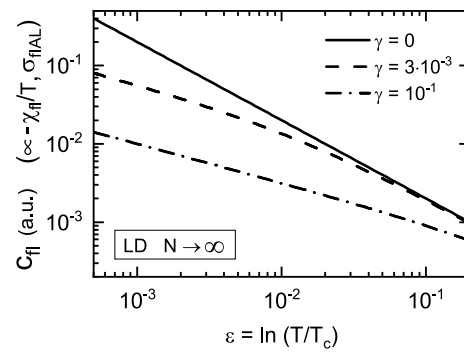


Fig. 2 Fluctuation specific heat c_{fl} from the well-known GGL-LD predictions for superconductors composed of an infinite number of parallel 2D planes, as a function of the reduced temperature ε and for different values of the Josephson-coupling constant γ between adjacent layers. (As a reference, for optimally-doped cuprates of the YBaCuO family values $\gamma \simeq 0.001 \sim 0.1$ are usually proposed [11–13]). The c_{fl} is given in arbitrary units, and is proportional to the also observables $-\chi_{fl}/T$ and σ_{fIAL} (see main text for details). The figure illustrates that when $\varepsilon \ll \gamma$ the c_{fl} behaves as in a 3D system (somewhat decreased amplitude and log-log slope $-1/2$) while if $\varepsilon \gg \gamma$ it displays a 2D behaviour (log-log slope -1). See also Fig. 3

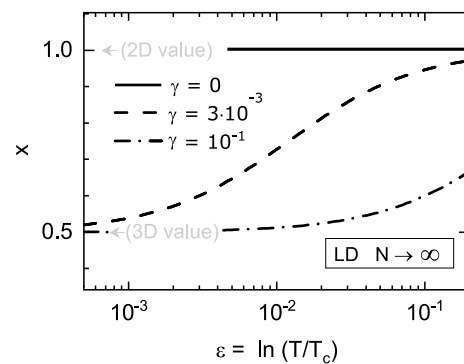


Fig. 3 Critical exponent x of c_{fl} (and of $-\chi_{fl}/T$ and σ_{fIAL}) resulting from the GGL-LD calculations for infinite-layers superconductors, as a function of the reduced temperature ε for different values of the Josephson coupling γ . The figure illustrates the crossover from the 3D value ($x = 1/2$) to the 2D one ($x = 1$) as ε evolves from $\varepsilon \ll \gamma$ to $\varepsilon \gg \gamma$, and that the dimensional crossover occurs around $\varepsilon_{crossover} \simeq 4\gamma$

T_c under zero external magnetic field c_{fl} may be written as [6, 10, 14, 15]:

$$c_{fl} = \frac{A_{TF}}{\varepsilon} \left(1 + \frac{B_{LD}}{\varepsilon} \right)^{-1/2}, \tag{1}$$

where $A_{TF} = k_B/[4\pi\xi_{ab}^2(0)s]$ is the Thouless-Ferrell amplitude [16, 17], $B_{LD} = [2\xi_c^2(0)/s]^2$ is the LD parameter [6, 10, 14, 15], s is the inter-layer distance and $\xi_{ab}(0)$ and $\xi_c(0)$ are the GL amplitudes of the coherence length in the in-plane and out-of-plane directions. The latter is given in terms

of the Josephson coupling constant between adjacent planes, γ , as $\xi_c(0) = s\sqrt{\gamma}$ [6, 10]. A representation of the resulting c_{fl} is given in Fig. 2. We also plot, in Fig. 3, the corresponding critical exponent (calculated from the log-log slope of the c_{fl} -vs- ε curve) showing that it crosses over the 2D ($x = 1$) and 3D ($x = 1/2$) values as ε decreases and T_c is approached [and as the inter-plane correlation grows by $\xi_c(\varepsilon) = \xi_c(0)\varepsilon^{-1/2}$; note that the crossover is located at around $\varepsilon_{\text{crossover}} \simeq B_{LD} = 4\gamma$.]

The LD calculations have been generalized by various authors to a number of different cases, including for instance non-Gaussian fluctuations [18, 19], inclusion of high-temperature effects [19–22], or also considering an infinite amount of layers but with two alternating inter-layer Josephson couplings γ_1 and γ_2 [6, 23, 24].

However, to our knowledge the critical fluctuations in superconductors composed of only a few layers [see Fig. 1 b, c] have not been calculated yet, even in the relatively simple Gaussian–Ginzburg–Landau (GGL) approximation above T_c . This will be the main purpose of the present work, with a focus on identifying possible dimensional crossover effects due to the Josephson couplings.

Let us note that a topic with some mathematical resemblance may be multi-band superconductors (with each band corresponding to the gap in different sheets of the Fermi surface) when Josephson-like expressions are chosen for the interband coupling. This case was considered in terms of fluctuations, e.g., in [25]. However, this is a different physical problem in various respects, the main ones being that such couplings do not introduce dimensional crossovers [25] (consequently with the fact that they do not correspond to spatial variations of the gaps) and that the interband interactions change T_c differently to the few-layer case [26–28].

In the present Topical Collection Article, we consider a GL functional of such a few-layer system and calculate the effects of critical fluctuations near but above the critical temperature, in the GGL approximation, for some of the main observables in the zero-external magnetic field limit (fluctuation heat capacity, magnetic susceptibility and electrical conductivity). We find explicit expression for various cases, and physically discuss the dimensional crossover effects induced by the inter-layer Josephson couplings in such geometries, focusing mainly in the two-layer and three-layer cases. Our results suggest that the finite-layer superconductors have the capability to display dimensional crossover effects quite comparable, in the variety of its phenomenology, to those in the LD model for infinite-layers superconductors. This includes, for instance, deviations from the 2D values of the critical exponents or crossovers of the amplitudes of the fluctuations when ε , and hence T/T_c , varies.

We organize this Topical Collection Article as follows: In Sect. 2 we write our basic equations and calculate the GGL fluctuation spectra. In Sect. 3 we write the resulting fluctuation contributions to three observables (the fluctuation specific heat, c_{fl} , the fluctuation-induced magnetic susceptibility, χ_{fl} , and the Aslamazov–Larkin electrical paraconductivity σ_{flAL}); we also write expressions for their corresponding critical exponents, x , and amplitudes, the latter through a so-called effective number of independent fluctuating planes N_e that will be helpful for the interpretation of the results. In Sect. 4 we discuss these results for two-layer superconductors in terms of their x and N_e crossovers as ε varies, for different Josephson couplings. In Sects. 5 and 6 we discuss the three-layer superconductors, for different values of the Josephson couplings and their ratio. In Sect. 7 we summarize our conclusions and briefly comment on some of the difficulties and challenges for further research in this topic.

2 Basic expressions for the Gaussian–Ginzburg–Landau fluctuations above T_c in two-layer and three-layer superconductors

2.1 GL functional

As starting point, let us model a superconductor composed by a (small) number N of parallel superconducting planes, each of them Josephson-coupled to its adjacent neighbour, by writing its Ginzburg–Landau (GL) functional as composed of the sum of free energies intrinsic to each $j = 1, \dots, N$ plane, plus interactions between each j and $j + 1$ planes:

$$\Delta F = \sum_{j=1}^N \Delta F_j^{\text{intr}} + \sum_{j=1}^{N-1} \Delta F_{jj+1}^{\text{inter}} \quad (2)$$

with

$$\Delta F_j^{\text{intr}} = a_0 \int d^2 r \left\{ \varepsilon_j |\psi_j|^2 + \frac{b}{2a_0} |\psi_j|^4 + \xi_{ab}^2(0) |\nabla_{xy} \psi_j|^2 \right\}, \quad (3)$$

where ψ_j are the GL wavefunctions of each plane, $r = (x, y)$ are the in-plane coordinates, and a_0 , b and $\xi_{ab}(0)$ are the GL constants and the in-plane coherence length amplitude. Also, ε_j is the reduced temperature of each plane:

$$\varepsilon_j = \ln(T/T_{c_j}) \simeq (T - T_{c_j})/T_{c_j}, \quad (4)$$

where T_{c_j} is its intrinsic critical temperature. In these initial equations we consider the general case in which T_{c_j} and ε_j may be different in each plane, but let us note already

here that many of our discussions in the present Topical Collection Article will focus, for concreteness, in the case in which all critical temperatures coincide ($T_{c_j} = T_c$, and hence also $\epsilon_j = \epsilon$, for all j). We also emphasize that we used the same $\xi_{ab}(0)$ for all the planes, which is probably a fair approximation if all of them are of the same material. Let us note that for most superconductors eventual variations of $\xi_{ab}(0)$ are linked to variations of T_c of greater extent, so that we expect that any eventual effects due to $\xi_{ab}(0)$ variations between layers are expected to be smaller than the corresponding effects due to different T_{c_j} .

For the inter-plane interaction term between planes j and $j + 1$ we employ (as is also done by the usual LD functional for infinite-layers superconductors):

$$\Delta F_{jj+1}^{inter} = a_0 \int d^2 r \{ \gamma_j |\psi_j - \psi_{j+1}|^2 \}, \tag{5}$$

where γ_j is a Josephson coupling constant between the planes j and $j + 1$. Note that in the limit $N \rightarrow \infty$ our functional given by Eqs. 2 to 5 simply recovers the usual LD functional for infinite-layers superconductors [10, 29]. Note also that we assumed, in Eqs. 3 and 5, zero external magnetic field and negligible effects of the potential vector gauge field (the latter would be important for the Kosterlitz-Thouless fluctuations below T_c). This is because we focus in this paper on $H = 0$ and for temperatures sufficiently above T_c as to be in the Gaussian–Ginzburg–Landau (GGL) region of the fluctuations. In that region, the $|\psi|^4$ term in Eq. 3 may be neglected and independent fluctuation modes, and their corresponding free energy, are searched. In the rest of this Topical Collection Article we proceed with that program for $N = 2$ and 3, and discuss the results.

2.2 GGL fluctuation modes for $N = 2$

In the $N = 2$ case, we have two (potentially different) intrinsic T_c 's, and hence two reduced temperatures ϵ_1 and ϵ_2 , and only one interlayer Josephson coupling constant $\gamma_1 = \gamma$. When considering this $N = 2$ case, the Eqs. 2 to 5 in the GGL approximation above T_c may be rewritten in explicit matrix form as:

$$\Omega(\psi_1, \psi_2) = (\psi_1^* \ \psi_2^*) \begin{pmatrix} \epsilon_1 + \gamma & -\gamma \\ -\gamma & \epsilon_2 + \gamma \end{pmatrix} \begin{pmatrix} \psi_1 \\ \psi_2 \end{pmatrix}, \tag{6}$$

where Ω is an interlayer contribution so that the total GL functional is:

$$\Delta F = a_0 \sum_{\alpha=Re,Im} \int d^2 r \left\{ \xi_{ab}^2(0) \sum_{j=1,2} |\nabla_{xy} \psi_j^\alpha|^2 + \Omega(\psi_1^\alpha, \psi_2^\alpha) \right\}. \tag{7}$$

In this expression it has been convenient to separate the wavefunctions into their real and imaginary parts, labeled by the index α . Note that Eq. 7 can be also written in k_{xy} -Fourier space as:

$$\Delta F \propto \sum_{\alpha=Re,Im} \int d k_x d k_y \left\{ \xi_{ab}^2(0) k_{xy}^2 \sum_{j=1,2} |\psi_{jk_{xy}}^\alpha|^2 + \Omega(\psi_{1k_{xy}}^\alpha, \psi_{2k_{xy}}^\alpha) \right\}. \tag{8}$$

We now diagonalize the 2×2 matrix in Eq. 6. This leads to

$$\Omega(\psi_1, \psi_2) = (f_1^* \ f_2^*) \begin{pmatrix} \omega_1 & 0 \\ 0 & \omega_2 \end{pmatrix} \begin{pmatrix} f_1 \\ f_2 \end{pmatrix}, \tag{9}$$

with

$$\omega_1 = \frac{1}{2} \left[\epsilon_1 + \epsilon_2 + 2\gamma - \sqrt{(\epsilon_1 - \epsilon_2)^2 + 4\gamma^2} \right], \tag{10}$$

$$\omega_2 = \frac{1}{2} \left[\epsilon_1 + \epsilon_2 + 2\gamma + \sqrt{(\epsilon_1 - \epsilon_2)^2 + 4\gamma^2} \right]. \tag{11}$$

The $f_{1,2}$ themselves are linear combinations of $\psi_{1,2}$ that in this small- N case may be expressed in a relatively compact form:

$$f_1 = \frac{(\omega_2 - \epsilon_1 - \gamma)\psi_1 + \gamma\psi_2}{\sqrt{(\omega_2 - \epsilon_1 - \gamma)^2 + \gamma^2}}, \tag{12}$$

$$f_2 = \frac{(\omega_1 - \epsilon_1 - \gamma)\psi_1 + \gamma\psi_2}{\sqrt{(\omega_1 - \epsilon_1 - \gamma)^2 + \gamma^2}}, \tag{13}$$

Note that in the limit of zero Josephson interplane coupling these quotients become simpler: In particular, for $\gamma \rightarrow 0$ it is $f_1 \rightarrow \psi_1$ and $f_2 \rightarrow \psi_2$ when $\epsilon_2 > \epsilon_1$, or $f_1 \rightarrow \psi_2$ and $f_2 \rightarrow -\psi_1$ when $\epsilon_1 > \epsilon_2$ (see next paragraph for the case $\epsilon_1 = \epsilon_2$; we used l'Hôpital's rule for the simultaneous zeroes in the numerator and denominator of Eqs. 12 and 13).

2.2.1 The case $N = 2$ with $T_{c1} = T_{c2} (= T_c)$

Let us here consider $N = 2$ but with all the planes having the same critical temperature, and hence also $\epsilon_1 = \epsilon_2 = \epsilon$. In that case, the inter-layer GGL energy eigenvalues ω_1 and ω_2 become:

$$\omega_1 = \epsilon, \tag{14}$$

$$\omega_2 = \epsilon + 2\gamma, \tag{15}$$

and the f_1, f_2 eigenwavefunctions are:

$$f_1 = (\psi_1 + \psi_2)/\sqrt{2}, \quad (16)$$

$$f_2 = (\psi_2 - \psi_1)/\sqrt{2}. \quad (17)$$

2.3 GGL fluctuation modes for $N = 3$

For $N = 3$, the matrix form of Ω becomes:

$$\Omega(\psi_1, \psi_2, \psi_3) = \begin{pmatrix} \psi_1^* & \psi_2^* & \psi_3^* \end{pmatrix} \begin{pmatrix} \varepsilon_1 + \gamma_1 & -\gamma_1 & 0 \\ -\gamma_1 & \varepsilon_2 + \gamma_1 + \gamma_2 & -\gamma_2 \\ 0 & -\gamma_2 & \varepsilon_3 + \gamma_2 \end{pmatrix} \begin{pmatrix} \psi_1 \\ \psi_2 \\ \psi_3 \end{pmatrix}. \quad (18)$$

Diagonalizing this matrix is possible with the use of Cardano's formulas for the roots of third order polynomials. The expression of the corresponding eigenvalues ω_1 to ω_3 are considerably long and therefore we devote Appendix 1 to write them. In the next subsection, we consider a more manageable case.

2.3.1 The case $N = 3$ with $T_{c1} = T_{c2} = T_{c3} (= T_c)$

Fortunately, the cumbersome general $N = 3$ expressions for $\omega_{1,2,3}$ dramatically collapse in size when considering the case in which all the planes share the same critical temperature. In this case, the inter-layer GGL energy eigenvalues simply become:

$$\omega_1 = \varepsilon, \quad (19)$$

$$\omega_2 = \varepsilon + \gamma_1 + \gamma_2 - \sqrt{\gamma_1^2 - \gamma_1\gamma_2 + \gamma_2^2}, \quad (20)$$

$$\omega_3 = \varepsilon + \gamma_1 + \gamma_2 + \sqrt{\gamma_1^2 - \gamma_1\gamma_2 + \gamma_2^2}, \quad (21)$$

where again $\varepsilon = \varepsilon_1 = \varepsilon_2 = \varepsilon_3$.

2.4 The quantity $\sum_{j=1}^N \omega_j^{-1}$

From such ω eigenvalues of the GGL functional, in principle most fluctuation-induced observables quantities may be obtained. In this regard, of particular significance will be the quantity $\sum \omega_j^{-1}$ because it will be proportional, in the GGL approach above T_c , to the fluctuation-induced heat capacity c_{fl} (see next Section; it will be also proportional to $-\chi_{fl}/T$ and σ_{flAL}) [6, 23].

In the $N = 2$ case with a single T_c , this quantity becomes:

$$\sum_{j=1}^2 \omega_j^{-1} = \frac{1}{\varepsilon} \frac{2\varepsilon + 2\gamma}{\varepsilon + 2\gamma}. \quad (22)$$

In the $N = 3$ case with a single T_c , it becomes:

$$\sum_{j=1}^3 \omega_j^{-1} = \frac{1}{\varepsilon} \frac{3\varepsilon^2 + 3\gamma_1\gamma_2 + 4\varepsilon(\gamma_1 + \gamma_2)}{\varepsilon^2 + 3\gamma_1\gamma_2 + 2\varepsilon(\gamma_1 + \gamma_2)}. \quad (23)$$

3 Fluctuation-induced heat capacity, magnetic susceptibility and AL paraconductivity

3.1 Expressions for c_{fl} , χ_{fl} and σ_{flAL}

From the GGL free energy written in terms of independent modes, it is possible to calculate its thermal statistical averages and then the fluctuation-induced contributions to various observables. In particular, for the basic averages of the independent modes, as expected it is $\langle |f_{j\kappa\lambda}^\alpha|^2 \rangle \propto k_B T / [\xi_{ab}^2(0)k_{xy}^2 + \omega_j]$, where not only the inter-plane contribution appears but also the in-plane kinetic energy term.¹ This is very similar to the case in the LD model, except for the substitution of the LD spectrum $\omega_{k_z}^{LD} = 2\gamma(1 - \cos k_z s)$ by our ω_j . Therefore it is easy to adapt to our case well-known LD calculations for the superconducting fluctuation contributions to various observables. In particular, for the following ones (always considered above T_c and in the limit of zero external magnetic field):

For the fluctuation-induced specific heat, c_{fl} (see, e.g., [6, 23] for a parallel calculation in the LD case):

$$c_{fl} = \frac{k_B}{4\pi\xi_{ab}^2(0)L_z} \sum_{j=1}^N \omega_j^{-1}, \quad (24)$$

where L_z is the thickness of the N -layer system.

For the fluctuation-induced magnetic susceptibility, χ_{fl} , with the magnetic field perpendicular to the layers and always in the weak magnetic field limit (see, e.g., [6] for a similar calculations in the LD case):

$$\frac{-\chi_{fl}}{T} = \frac{\mu_0\pi k_B \xi_{ab}^2(0)}{3\phi_0^2 L_z} \sum_{j=1}^N \omega_j^{-1}. \quad (25)$$

For the in-plane electrical conductivity, we also calculated (adapting the procedures of [6, 7, 23]) the direct fluctuation contribution (also known as Aslamazov–Larkin paraconductivity σ_{flAL}), that is the dominant contribution to the experimental σ_{fl} at least in high-temperature cuprates [11–13]:²

¹ In our expressions k_B , μ_0 , ϕ_0 , e and \hbar are the usual universal physical constants.

² For σ_{flAL} , we are assuming a sample with enough distance between electrical contacts for the inter-plane *resistance* to be well smaller than the in-plane one, so that all layers must be averaged in

$$\sigma_{fIAL} = \frac{e^2}{16\hbar L_z} \sum_{j=1}^N \omega_j^{-1}. \tag{26}$$

When combined with our explicit formulae for the quantity $\sum \omega_j^{-1}$ for $N = 2$ and $N = 3$ (Eqs. 22 and 23), the above expressions for c_{fl} , χ_{fl} and σ_{fIAL} become also explicit.

3.2 Critical exponents

In order to physically discuss the above results for c_{fl} , χ_{fl} and σ_{fIAL} , a first quantity of interest will be the critical exponent, defined from the log-log slope of the plot of the fluctuation heat capacity versus reduced-temperature:

$$x = -\frac{\partial \ln c_{fl}}{\partial \ln \varepsilon}. \tag{27}$$

Note that the same critical exponent is going to be shared with $-\chi_{fl}/T$ and σ_{fIAL} . Note also that in the 2D limit it is $c_{fl} \propto \varepsilon^{-1}$ and therefore $x = 1$ (while for 3D bulks it is $x = 1/2$).

When applied to the Eqs. 22 to 24 obtained in the previous sections, Eq. 27 leads to the following result for the $N = 2$ case:

$$x = \frac{\varepsilon^2 + 2\gamma\varepsilon + 2\gamma^2}{(\varepsilon + \gamma)(\varepsilon + 2\gamma)}, \tag{28}$$

and for the $N = 3$ case:

$$x = \frac{3\varepsilon^4 + 8(\gamma_1 + \gamma_2)\varepsilon^3 + 8(\gamma_1 + \gamma_2)^2\varepsilon^2 + 12\gamma_1\gamma_2(\gamma_1 + \gamma_2)\varepsilon + 9\gamma_1^2\gamma_2^2}{[\varepsilon^2 + 3\gamma_1\gamma_2 + 2\varepsilon(\gamma_1 + \gamma_2)] [3\varepsilon^2 + 3\gamma_1\gamma_2 + 4\varepsilon(\gamma_1 + \gamma_2)]}. \tag{29}$$

Both of these expressions saturate to the pure 2D value $x = 1$ in the limit of zero Josephson coupling between planes ($\gamma_j \rightarrow 0$), as it could be expected.

3.3 Effective number of independently fluctuating planes

We also introduce now a second relevant quantity, informing about the amplitude of the fluctuations. We shall call this the “effective number of independently fluctuating superconducting planes”, N_e , and we define it as

$$N_e = \frac{c_{fl}}{c_{fl}^{N=1}} = \frac{\chi_{fl}}{\chi_{fl}^{N=1}} = \frac{\sigma_{fIAL}}{\sigma_{fIAL}^{N=1}}. \tag{30}$$

In other words, this quantity is the increment of the fluctuations with respect to the value expected for a $N = 1$ 2D

layer (with the same L_z). A value $N_e = 1$ would indicate all of the N planes are fluctuating together as a single plane, and is expected to correspond at least to the limit $\gamma \rightarrow \infty$ (strong inter-plane correlation). In contrast, a value $N_e = N$ is expected to be recovered at least in the limit $\gamma \rightarrow 0$ (no inter-plane correlations, each plane fluctuates independently of the other).

4 Discussion of the results for two-layer superconductors

Let us now present a more physical discussion of the consequences of the expressions obtained up to now, starting here with the simpler $N = 2$ case (we defer $N = 3$ to the Sects. 5 and 6).

We first note that in this $N = 2$ case the interlayer fluctuation energy is split into two contributions, the ones of Eqs. 14 and 15, what may be understood as one half of the fluctuation modes having the same energy as in a regular 2D layer, and the other half having the fluctuation energy of a 2D layer but with an “effective” reduced temperature $\varepsilon + 2\gamma$ [or with effective critical temperature $T_c / \exp(2\gamma)$]. Logically, the total fluctuation superfluid density accumulates both contributions, and so does $c_{fl}^{N=2}$ (via the quantity $\sum \omega_j^{-1}$).

In the case $\gamma = 0$ (no interlayer interactions) both independent modes behave with the same effective critical temperature. In that case, as it could be expected the critical exponent is the 2D value, $x = 1$, and the effective number of independently fluctuating planes becomes $N_e = 2$:

$$N_e(\gamma = 0) = 2, \tag{31}$$

$$x(\gamma = 0) = 1. \tag{32}$$

In the case with $\gamma \rightarrow \infty$ we expect however the two planes acting as a single one, and in fact in that limit we get:

$$N_e(\gamma \rightarrow \infty) = 1, \tag{33}$$

$$x(\gamma \rightarrow \infty) = 1. \tag{34}$$

Note that the limit $\gamma \rightarrow \infty$ has the physical meaning that any variation of the superconducting wave function between adjacent layers would be energetically prohibitive, so that the only physically relevant situation in the statistical averages would be having the two layers acting as a single one - what directly should imply $x = 1$ and $N_e = 1$, as the above equations confirm. (These equations can be also understood by considering that if $\gamma \rightarrow \infty$ the f_2 fluctuating mode becomes too difficult to excite and does not contribute to c_{fl}).

Footnote 2 (continued)

the conduction. This is generally the case expected in experiments with real few-layer films.

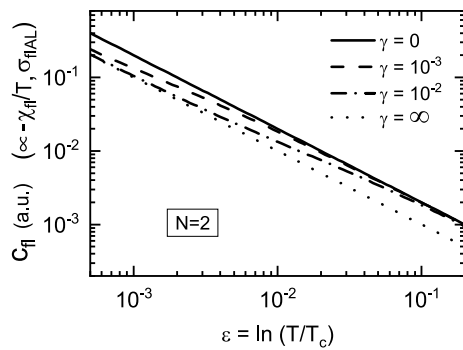


Fig. 4 Fluctuation specific heat c_{fl} from our expressions for two-layer superconductors, as a function of the reduced temperature ε and for different values of the Josephson coupling γ . The c_{fl} is given in arbitrary units (and is proportional to the also observables $-\chi_{fl}/T$ and σ_{flAL}). See also Figs. 5 and 6 for an interpretation of the results

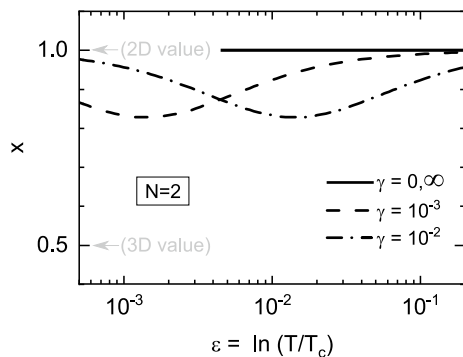


Fig. 5 Critical exponent x of c_{fl} (and of $-\chi_{fl}/T$ and σ_{flAL}) for two-layer superconductors, as a function of ε and for different γ . The figure illustrates deviations from the 2D value ($x = 1$) when ε and γ take comparable values, which may be further understood when contrasted with the N_e evolution in Fig. 6

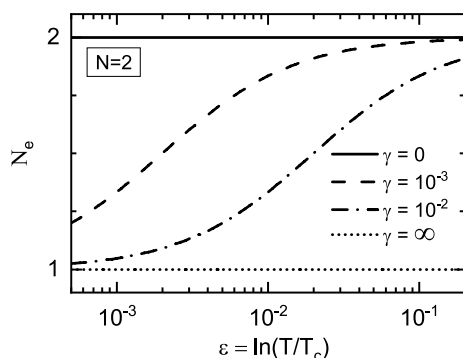


Fig. 6 Effective number of independent fluctuating planes, N_e , for two-layer superconductors, as a function of ε and for different γ . The figure illustrates crossovers between the $N_e = 1$ and 2 values as ε and γ vary, and with them the corresponding inter-plane correlations. These crossovers may be correlated with the evolutions of the critical exponent x in Fig. 5

Between these two pure 2D limits ($x = 1$ with either $N_e = 1$ or 2) intermediate cases must appear, in which the inter-plane correlations will result in deviations of the critical exponent from the 2D value, $x \neq 1$. Also, N_e must undergo a crossover between $N_e = 2$ and $N_e = 1$ as γ evolves from 0 to ∞ . This is represented in Figs. 4, 5 and 6. In particular, Fig. 6 plots $N_e^{N=2}$ versus ε for different values of the inter-layer coupling γ . For $\gamma \rightarrow \infty$ and $\gamma = 0$, the limiting values 1 and 2 are obtained, as commented before. For intermediate γ values, also $N_e \rightarrow 1$ if $\varepsilon \rightarrow 0$. This agrees with the fact that when $\varepsilon \rightarrow 0$ both planes are expected to be strongly correlated due to the growth (and divergence at $T = T_c$) of the coherence length between them (that may be estimated as $\xi_c(\varepsilon) = \xi_c(0)/\sqrt{\varepsilon}$ with $\xi_c(0) = L_z/\sqrt{\gamma}$, in analogy to the usual LD model for infinite-layers superconductors). In contrast, as $\varepsilon \rightarrow \infty$ and $\xi_c(\varepsilon) \rightarrow 0$ both planes will become progressively independent and $N_e = N (= 2$ in this case), as confirmed by Fig. 6. A rough estimate of the midpoint of this N_e crossover may be obtained from $\xi_c(\varepsilon) \sim L_z$, again in analogy to what occurs in the LD model. This leads to $\varepsilon_{\text{crossover}} \sim \gamma$, in good agreement with Fig. 5.

In Fig. 5, it may be observed a phenomenology for the critical exponent x that is consequent with the above considerations. In particular, for both $\gamma = 0$ and $\gamma \rightarrow \infty$ a pure 2D value $x = 1$ is obtained (irrespectively of $N_e = 1$ or 2 the system behaves as a planar one). This pure 2D exponent is also obtained for intermediate values of γ when either $\varepsilon \rightarrow 0$ or $\varepsilon \rightarrow \infty$, corresponding to the fact that also $N_e \rightarrow 1$ or 2. But when both γ and ε have intermediate values, a deviation from the pure 2D behaviour appears, indicating precursor correlations in the third dimension. Then, x becomes intermediate between the 2D and 3D values ($x = 1$ and $1/2$). In fact, the minimum of $x(\varepsilon)$, calculable by $\partial x/\partial \varepsilon = 0$, just happens at $\varepsilon_{\text{crossover}} = \sqrt{2}\gamma$, corresponding to $x \approx 0.83$, which is similar to what was estimated above for the N_e crossover. Therefore, we conclude that this $N = 2$ finite layer case has a capability of displaying intermediate-dimensionality crossover not very far from what happens in the infinite-layers case, although without the capability of reaching the 3D limit.

5 Discussion of the results for three-layer superconductors with $\gamma_1 = \gamma_2 (= \gamma)$

We now explore the physical consequences of the expressions obtained for the $N = 3$ case. For concreteness, we first consider the case in which γ_1 and γ_2 take a common value γ (in the Sect. 6 we shall consider the $\gamma_1 \neq \gamma_2$ case). As in the $N = 2$ case, the relevant quantities will be c_{fl} , N_e and x .

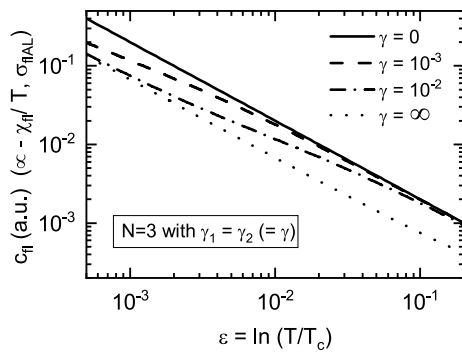


Fig. 7 Fluctuation specific heat c_{fi} from our expressions for three-layer superconductors with a single Josephson coupling, $\gamma = \gamma_1 = \gamma_2$, as a function of the reduced temperature ϵ and for different γ . The c_{fi} is given in arbitrary units (and is proportional to the also observables $-\chi_{fi}/T$ and σ_{fiAL}). See also Figs. 8 and 9 for an interpretation of the results

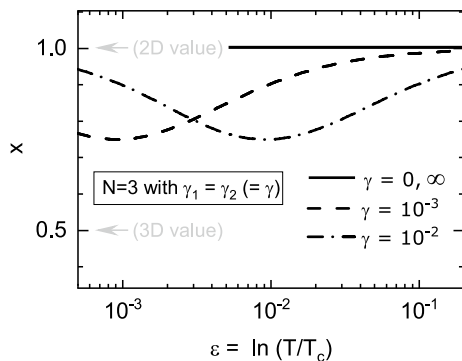


Fig. 8 Critical exponent x of c_{fi} (and of $-\chi_{fi}/T$ and σ_{fiAL}) for three-layer superconductors with a single Josephson coupling, $\gamma = \gamma_1 = \gamma_2$, as a function of ϵ and for different γ . The figure illustrates deviations from the 2D value ($x = 1$) when ϵ and γ take comparable values, which may be further understood when contrasted with the N_e evolution in Fig. 9

First of all, note that when $\gamma = 0$ we obtain the expected 2D result ($x = 1$), with $N_e = 3$ as also expected (each plane behaves independently and acts twodimensionally):

$$N_e(\gamma_1 = \gamma_2 = 0) = 3, \tag{35}$$

$$x(\gamma_1 = \gamma_2 = 0) = 1. \tag{36}$$

The equations also reproduce the expected result for the opposite limit $\gamma \rightarrow \infty$, in which the three planes should act as a single one. In that case, the equations produce $x = 1$ and $N_e = 1$ as it corresponds to that physical situation:

$$N_e(\gamma_1 = \gamma_2 \rightarrow \infty) = 1, \tag{37}$$

$$x(\gamma_1 = \gamma_2 \rightarrow \infty) = 1. \tag{38}$$

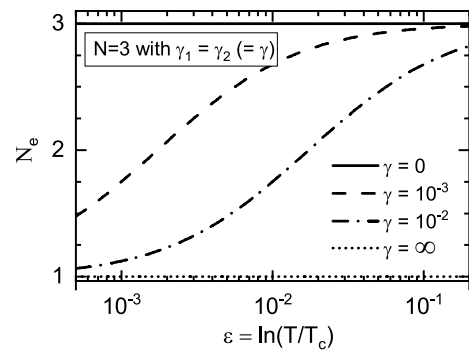


Fig. 9 Effective number of independent fluctuating planes, N_e , for three-layer superconductors with a single Josephson coupling, $\gamma = \gamma_1 = \gamma_2$, as a function of ϵ and for different γ . The figure illustrates crossovers between the $N_e = 1$ and 3 values (with no plateau at $N_e \simeq 2$) as ϵ and γ vary (and with them the corresponding inter-plane correlations) correlated with the evolutions of the critical exponent x in Fig. 8

Between these two pure 2D limits, intermediate-dimensionality cases must appear for intermediate values of γ . This is represented in Figs. 7, 8 and 9. In Fig. 9, N_e is plotted versus ϵ for different values of γ . As expected, there is a crossover as ϵ increases from $N_e = 1$ up to $N_e = 3$. The crossover temperature increases as γ decreases (and for $\gamma = 0$ or $\gamma \rightarrow \infty$ the crossover is outside of the experimental window). In Fig. 8 the critical exponent x is plotted versus reduced temperature. Again, the $x(\epsilon)$ behaviour is correlated with the evolution of N_e : When $N_e = 1$ or 3, x takes the 2D value $x = 1$, and when N_e is crossing over those values the system develops a non-2D critical exponent (becoming closer to the 3D value the further away N_e is from its limiting values 1 or 3).

6 Discussion of the results for three-layer superconductors with $\gamma_1 > \gamma_2$

We now explore the case $N = 3$ with significantly different interlayer Josephson couplings γ_1 and γ_2 . For concreteness, we take $\gamma_1/\gamma_2 > 1$ (but note that the equations are symmetrical to interchanges of γ_1 and γ_2).

Figures 10, 11 and 12 [panels (a) for $\gamma_1/\gamma_2 = 100$ and panels (b) for $\gamma_1/\gamma_2 = 1000$] display the c_{fi} , x and N_e versus reduced temperature obtained for $N = 3$ and different values of γ_2 .

As it happened in the previous Section, for $\gamma_2 = 0$ and $\gamma_2 \rightarrow \infty$ two different 2D limit cases are obtained, with $x = 1$ and $N_e = N = 3$ for $\gamma_2 = 0$, and with $x = 1$ and $N_e = 1$ for $\gamma_1 \rightarrow \infty$.

Intermediate dimensionality behaviour appears for intermediate values of γ_2 (and hence γ_1), in which x may develop deviations from the 2D value simultaneously

Fig. 10 Panel **a** Fluctuation specific heat c_{fl} from our expressions for three-layer superconductors with different Josephson couplings $\gamma_1/\gamma_2 = 100$, as a function of the reduced temperature ε and for different values of γ_2 . Panel **b** Same for an increased $\gamma_1/\gamma_2 = 1000$. See also Figs. 11 and 12 for an interpretation of the results

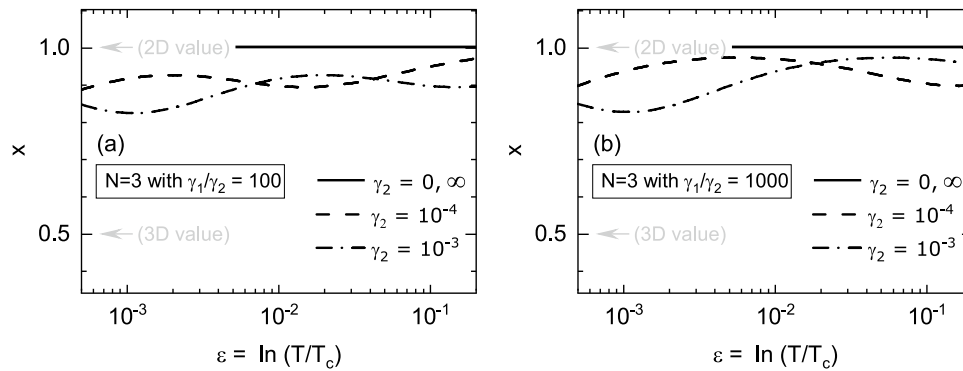
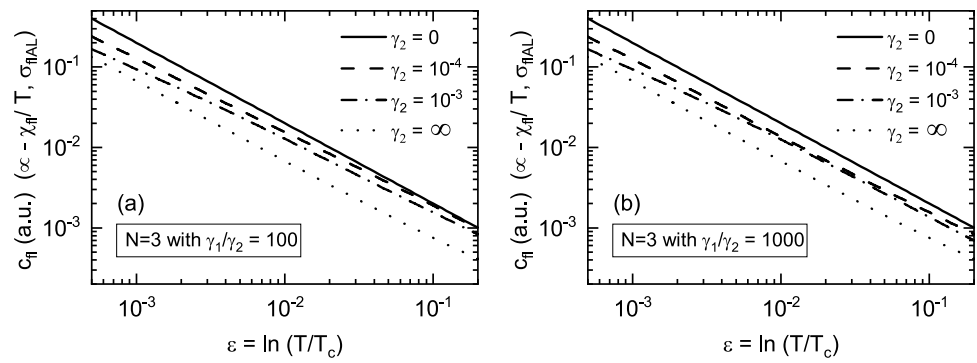


Fig. 11 Panel **a** Critical exponent x of c_{fl} for three-layer superconductors with $\gamma_1/\gamma_2 = 100$, as a function of ε and for different γ_2 . The figure hints at double-featured deviations from the 2D value ($x = 1$) which may be correlated with the N_e changes (and pla-

teaus) in Fig. 12 (see also main text). Panel **b** Same for an increased $\gamma_1/\gamma_2 = 1000$, illustrating a softening (rather than a displacement) of the $x \neq 1$ features

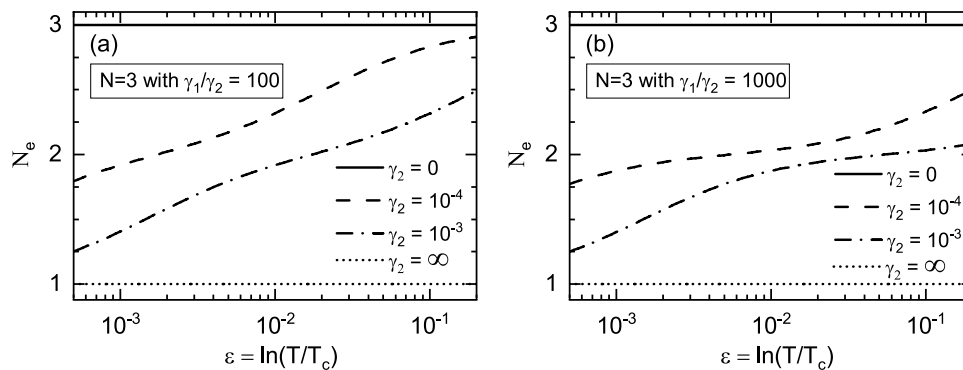


Fig. 12 Panel **a** Effective number of independent fluctuating planes, N_e , for three-layer superconductors with $\gamma_1/\gamma_2 = 100$, as a function of ε and for different γ_2 . The figure illustrates not only a crossover between $N_e = 1$ and 3, but also a small plateau around

$N_e \approx 2$. Panel **b** Same for $\gamma_1/\gamma_2 = 1000$, demonstrating an enlargement of the plateau around $N_e \approx 2$ (correlated to the softening of the $x \neq 1$ features in Fig. 11)

to deviations of N_e from its saturation values 1 or 3. But an interesting additional feature may appear at certain reduced temperatures, in which N_e plateaus at $N_e = 2$. This must correspond to the case in which two of the layers have already saturated their mutual correlation, while the third still develops fluctuations not locked to the ones of

the other layers. This feature may be seen in our Figs. 10, 11 and 12, mainly in those corresponding to $\gamma_1/\gamma_2 = 1000$ [i.e., panels (b)], while for the lower $\gamma_1/\gamma_2 = 100$ the N_e plateau is well smaller. The resulting evolution of $x(\varepsilon)$ becomes then of non-trivial aspect (also for $\gamma_1/\gamma_2 = 100$), though it may be understood as a double valley of deepness tracking

the slope of $N_e(\epsilon)$. We conclude therefore that this $N = 3$ case not only is able to display intermediate dimensionality behaviour in comparable significance to the infinite-layers case, but also that this case is to some extent able to display richer phenomenology (multiple crossovers) in spite of never reaching true 3D ($x = 1/2$) behaviour.

7 Conclusions and some remaining challenges

In conclusion, we have considered a GL functional of a few-layer superconductor (mainly two- and three-layer) and calculated the effects of critical fluctuations above the critical temperature, in the GGL approximation, for some of the main observables in the zero-external magnetic field limit (fluctuation heat capacity, magnetic susceptibility and electrical conductivity). The resulting expressions suggest the capability of these systems to display crossover effects on the critical exponents and amplitudes, with similarities and differences with respect to those predicted by the Lawrence–Doniach (LD) model for infinite-layers superconductors. For instance, in the bi-layer ($N = 2$) case the critical exponent develops deviations from the pure 2D value as the temperature approaches T_c (as in the LD model) but, instead of crossing over from the 2D to the 3D values (see Fig. 3), it undergoes a different evolution (see Fig. 5) of critical spatial dimensionality (2D - intermediate dimensionality - 2D), including two 2D regimes with different effective number of independently fluctuating planes (see Fig. 6). Also, for $N = 3$ the evolution of the critical exponent displays a similar frustrated change of dimensionality plus an evolution of the number of independent layers from $N_e = 1$ to $N_e = 3$.

Let us finally briefly comment on some of the expected challenges and difficulties on further studying these potentially interesting superconducting fluctuations of few-layer systems. First, in spite of sample availability now being far easier than in the past [1–4], the specimens are bound to be small in volume; this could make measurements of the heat capacity challenging, probably favouring magnetic screening or electrical measurements (and hence χ and/or σ). Smallness also makes boundary conditions more important, and while for negligible external magnetic fields and above the transition (the case studied in this Topical Collection Article) a change in the value of T_c may be expected to roughly summarize most of these boundary effects, for other situations involving well-developed vortices (sizeable magnetic fields, temperatures below the transition, etc.) the constraints imposed by the

substrate of the sample will have to be taken into account, both experimentally and theoretically. Also, because of these substrate effects and other issues, it could be important to further extend our calculations to the case with different T_c for each plane, only hinted at in the present article. Probably more challenging may be to extend them to the case with larger number of planes, as the difficulty of the matrix diagonalization increases considerably with N , what could constraint calculations to be only numerical instead of analytical.

Acknowledgements This work was supported by the Agencia Estatal de Investigación (AEI) and Fondo Europeo de Desarrollo Regional (FEDER) through project PID2019-104296GB-I00, by Xunta de Galicia (grant GRC number ED431C 2018/11) and iMATUS (2021 internal project RL3). JCV was supported by the Spanish Ministry of Education for Grant FPU14/00838. MMB was supported by Ministerio de Universidades of Spain through the National Program FPU (Grant Number FPU19/05266).

Data availability The Article has no associated data.

Declarations

Conflict of interest The authors of this paper declare that they have no conflict of interest.

Open Access This article is licensed under a Creative Commons Attribution 4.0 International License, which permits use, sharing, adaptation, distribution and reproduction in any medium or format, as long as you give appropriate credit to the original author(s) and the source, provide a link to the Creative Commons licence, and indicate if changes were made. The images or other third party material in this article are included in the article's Creative Commons licence, unless indicated otherwise in a credit line to the material. If material is not included in the article's Creative Commons licence and your intended use is not permitted by statutory regulation or exceeds the permitted use, you will need to obtain permission directly from the copyright holder. To view a copy of this licence, visit <http://creativecommons.org/licenses/by/4.0/>

Appendix 1: Full expression for ω_j in the $N = 3$ case

The following are the complete expressions for the fluctuation energy spectrum for $N = 3$ and arbitrary $\epsilon_1, \epsilon_2, \epsilon_3, \gamma_1$ and γ_2 :

$$\begin{aligned} \omega_3 = & 1/3(\varepsilon_1 + \varepsilon_2 + \varepsilon_3 + 2\gamma_1 + 2\gamma_2) \\ & + ((1 - i\sqrt{3})(-\varepsilon_1 - \varepsilon_2 - \varepsilon_3 - 2\gamma_1 - 2\gamma_2)^2 \\ & + 3(\varepsilon_1\varepsilon_2 + \varepsilon_1\varepsilon_3 + \varepsilon_2\varepsilon_3 + \varepsilon_1\gamma_1 + \varepsilon_2\gamma_1 + 2\varepsilon_3\gamma_1 \\ & + 2\varepsilon_1\gamma_2 + \varepsilon_2\gamma_2 + \varepsilon_3\gamma_2 + 3\gamma_1\gamma_2)) / (3 \cdot 2^{2/3}(2\varepsilon_1^3 \\ & - 3\varepsilon_1^2\varepsilon_2 - 3\varepsilon_1\varepsilon_2^2 + 2\varepsilon_2^3 - 3\varepsilon_1^2\varepsilon_3 + 12\varepsilon_1\varepsilon_2\varepsilon_3 \\ & - 3\varepsilon_2^2\varepsilon_3 - 3\varepsilon_1\varepsilon_3^2 - 3\varepsilon_2\varepsilon_3^2 + 2\varepsilon_3^3 + 3\varepsilon_1^2\gamma_1 \\ & - 12\varepsilon_1\varepsilon_2\gamma_1 + 3\varepsilon_2^2\gamma_1 + 6\varepsilon_1\varepsilon_3\gamma_1 + 6\varepsilon_2\varepsilon_3\gamma_1 - 6\varepsilon_3^2\gamma_1 \\ & + 6\varepsilon_1\gamma_1^2 + 6\varepsilon_2\gamma_1^2 - 12\varepsilon_3\gamma_1^2 + 16\gamma_1^3 - 6\varepsilon_1^2\gamma_2 \\ & + 6\varepsilon_1\varepsilon_2\gamma_2 + 3\varepsilon_2^2\gamma_2 + 6\varepsilon_1\varepsilon_3\gamma_2 - 12\varepsilon_2\varepsilon_3\gamma_2 \\ & + 3\varepsilon_3^2\gamma_2 - 6\varepsilon_1\gamma_1\gamma_2 + 12\varepsilon_2\gamma_1\gamma_2 - 6\varepsilon_3\gamma_1\gamma_2 - 6\gamma_1^2\gamma_2 \\ & - 12\varepsilon_1\gamma_2^2 + 6\varepsilon_2\gamma_2^2 + 6\varepsilon_3\gamma_2^2 - 6\gamma_1\gamma_2^2 + 16\gamma_2^3 + ((2\varepsilon_1^3 \\ & - 3\varepsilon_1^2\varepsilon_2 - 3\varepsilon_1\varepsilon_2^2 + 2\varepsilon_2^3 - 3\varepsilon_1^2\varepsilon_3 + 12\varepsilon_1\varepsilon_2\varepsilon_3 \\ & - 3\varepsilon_2^2\varepsilon_3 - 3\varepsilon_1\varepsilon_3^2 - 3\varepsilon_2\varepsilon_3^2 + 2\varepsilon_3^3 + 3\varepsilon_1^2\gamma_1 \\ & - 12\varepsilon_1\varepsilon_2\gamma_1 + 3\varepsilon_2^2\gamma_1 + 6\varepsilon_1\varepsilon_3\gamma_1 + 6\varepsilon_2\varepsilon_3\gamma_1 \\ & - 6\varepsilon_3^2\gamma_1 + 6\varepsilon_1\gamma_1^2 + 6\varepsilon_2\gamma_1^2 - 12\varepsilon_3\gamma_1^2 + 16\gamma_1^3 - 6\varepsilon_1^2\gamma_2 \\ & + 6\varepsilon_1\varepsilon_2\gamma_2 + 3\varepsilon_2^2\gamma_2 + 6\varepsilon_1\varepsilon_3\gamma_2 - 12\varepsilon_2\varepsilon_3\gamma_2 \\ & + 3\varepsilon_3^2\gamma_2 - 6\varepsilon_1\gamma_1\gamma_2 + 12\varepsilon_2\gamma_1\gamma_2 - 6\varepsilon_3\gamma_1\gamma_2 \\ & - 6\gamma_1^2\gamma_2 - 12\varepsilon_1\gamma_2^2 + 6\varepsilon_2\gamma_2^2 + 6\varepsilon_3\gamma_2^2 - 6\gamma_1\gamma_2^2 + 16\gamma_2^3))^2 \\ & + 4(-(\varepsilon_1 - \varepsilon_2 - \varepsilon_3 - 2\gamma_1 - 2\gamma_2)^2 + 3(\varepsilon_1\varepsilon_2 + \varepsilon_1\varepsilon_3 \\ & + \varepsilon_2\varepsilon_3 + \varepsilon_1\gamma_1 + \varepsilon_2\gamma_1 + 2\varepsilon_3\gamma_1 + 2\varepsilon_1\gamma_2 + \varepsilon_2\gamma_2 \\ & + \varepsilon_3\gamma_2 + 3\gamma_1\gamma_2))^3)^{1/2})^{1/3} - (1/(6 \cdot 2^{1/3})) \\ & (1 + i\sqrt{3})(2\varepsilon_1^3 - 3\varepsilon_1^2\varepsilon_2 \\ & - 3\varepsilon_1\varepsilon_2^2 + 2\varepsilon_2^3 - 3\varepsilon_1^2\varepsilon_3 + 12\varepsilon_1\varepsilon_2\varepsilon_3 - 3\varepsilon_2^2\varepsilon_3 \\ & - 3\varepsilon_1\varepsilon_3^2 - 3\varepsilon_2\varepsilon_3^2 + 2\varepsilon_3^3 + 3\varepsilon_1^2\gamma_1 - 12\varepsilon_1\varepsilon_2\gamma_1 \\ & + 3\varepsilon_2^2\gamma_1 + 6\varepsilon_1\varepsilon_3\gamma_1 + 6\varepsilon_2\varepsilon_3\gamma_1 - 6\varepsilon_3^2\gamma_1 \\ & + 6\varepsilon_1\gamma_1^2 + 6\varepsilon_2\gamma_1^2 - 12\varepsilon_3\gamma_1^2 + 16\gamma_1^3 - 6\varepsilon_1^2\gamma_2 \\ & + 6\varepsilon_1\varepsilon_2\gamma_2 + 3\varepsilon_2^2\gamma_2 + 6\varepsilon_1\varepsilon_3\gamma_2 - 12\varepsilon_2\varepsilon_3\gamma_2 \\ & + 3\varepsilon_3^2\gamma_2 - 6\varepsilon_1\gamma_1\gamma_2 + 12\varepsilon_2\gamma_1\gamma_2 - 6\varepsilon_3\gamma_1\gamma_2 - 6\gamma_1^2\gamma_2 \\ & - 12\varepsilon_1\gamma_2^2 + 6\varepsilon_2\gamma_2^2 + 6\varepsilon_3\gamma_2^2 - 6\gamma_1\gamma_2^2 + 16\gamma_2^3 + ((2\varepsilon_1^3 \\ & - 3\varepsilon_1^2\varepsilon_2 - 3\varepsilon_1\varepsilon_2^2 + 2\varepsilon_2^3 - 3\varepsilon_1^2\varepsilon_3 + 12\varepsilon_1\varepsilon_2\varepsilon_3 \\ & - 3\varepsilon_2^2\varepsilon_3 - 3\varepsilon_1\varepsilon_3^2 - 3\varepsilon_2\varepsilon_3^2 + 2\varepsilon_3^3 + 3\varepsilon_1^2\gamma_1 \\ & - 12\varepsilon_1\varepsilon_2\gamma_1 + 3\varepsilon_2^2\gamma_1 + 6\varepsilon_1\varepsilon_3\gamma_1 + 6\varepsilon_2\varepsilon_3\gamma_1 \\ & - 6\varepsilon_3^2\gamma_1 + 6\varepsilon_1\gamma_1^2 + 6\varepsilon_2\gamma_1^2 - 12\varepsilon_3\gamma_1^2 + 16\gamma_1^3 - 6\varepsilon_1^2\gamma_2 \\ & + 6\varepsilon_1\varepsilon_2\gamma_2 + 3\varepsilon_2^2\gamma_2 + 6\varepsilon_1\varepsilon_3\gamma_2 - 12\varepsilon_2\varepsilon_3\gamma_2 \\ & + 3\varepsilon_3^2\gamma_2 - 6\varepsilon_1\gamma_1\gamma_2 + 12\varepsilon_2\gamma_1\gamma_2 - 6\varepsilon_3\gamma_1\gamma_2 - 6\gamma_1^2\gamma_2 \\ & - 12\varepsilon_1\gamma_2^2 + 6\varepsilon_2\gamma_2^2 + 6\varepsilon_3\gamma_2^2 - 6\gamma_1\gamma_2^2 + 16\gamma_2^3))^2 \\ & + 4(-(\varepsilon_1 - \varepsilon_2 - \varepsilon_3 - 2\gamma_1 - 2\gamma_2)^2 \\ & + 3(\varepsilon_1\varepsilon_2 + \varepsilon_1\varepsilon_3 + \varepsilon_2\varepsilon_3 \\ & + \varepsilon_1\gamma_1 + \varepsilon_2\gamma_1 + 2\varepsilon_3\gamma_1 + 2\varepsilon_1\gamma_2 + \varepsilon_2\gamma_2 + \varepsilon_3\gamma_2 \\ & + 3\gamma_1\gamma_2))^3)^{1/2})^{1/3} \end{aligned}$$

Appendix 2: Expressions for ω_j in the $N = 4$, $N = 5$ and $N = 6$ cases, with a single T_c and Josephson coupling

In the main text of this Topical Collection Article we have focused on the $N = 2$ and $N = 3$ cases, because they are analytically solvable and relatively manageable. Here, let us briefly comment on the $N > 3$ cases. Their main difficulty is to solve the eigenvalue problem of the corresponding $N \times N$ matrix, and associated N^{th} order polynomial equation. In general this is not feasible for $N > 3$. However, we found that in the case $\varepsilon_1 = \varepsilon_2 = \dots \varepsilon_N$ and $\gamma_1 = \gamma_2 = \dots \gamma_{N-1}$ (i.e., a single T_c and Josephson coupling) it is possible to rewrite the $N = 4, 5$ and 6 polynomials in a solvable form (we were unable to solve the $N = 7$ case). We provide those solutions in this Appendix.

For $N = 4$ and $\varepsilon_1 = \varepsilon_2 = \varepsilon_3 = \varepsilon_4 (= \varepsilon)$ and $\gamma_1 = \gamma_2 = \gamma_3 = \gamma_4 (= \gamma)$, we found:

$$\omega_1 = \varepsilon \tag{39}$$

$$\omega_2 = \varepsilon + 2\gamma \tag{40}$$

$$\omega_3 = \varepsilon + 2\gamma - \sqrt{2}\gamma \tag{41}$$

$$\omega_4 = \varepsilon + 2\gamma + \sqrt{2}\gamma \tag{42}$$

For $N = 5$ and $\varepsilon_1 = \varepsilon_2 = \dots \varepsilon_5 (= \varepsilon)$ and $\gamma_1 = \gamma_2 = \dots \gamma_5 (= \gamma)$, we found:

$$\omega_1 = \varepsilon \tag{43}$$

$$\omega_2 = \frac{1}{2}(2\varepsilon + 3\gamma - \sqrt{5}\gamma) \tag{44}$$

$$\omega_3 = \frac{1}{2}(2\varepsilon + 5\gamma - \sqrt{5}\gamma) \tag{45}$$

$$\omega_4 = \frac{1}{2}(2\varepsilon + 3\gamma + \sqrt{5}\gamma) \tag{46}$$

$$\omega_5 = \frac{1}{2}(2\varepsilon + 5\gamma + \sqrt{5}\gamma) \tag{47}$$

For $N = 6$ and $\varepsilon_1 = \varepsilon_2 = \dots \varepsilon_6 (= \varepsilon)$ and $\gamma_1 = \gamma_2 = \dots \gamma_6 (= \gamma)$, we found:

$$\omega_1 = \varepsilon \tag{48}$$

$$\omega_2 = \varepsilon + \gamma \tag{49}$$

$$\omega_3 = \varepsilon + 2\gamma \tag{50}$$

$$\omega_4 = \varepsilon + 3\gamma \quad (51)$$

$$\omega_5 = \varepsilon + 2\gamma - \sqrt{3}\gamma \quad (52)$$

$$\omega_6 = \varepsilon + 2\gamma + \sqrt{3}\gamma \quad (53)$$

References

- Bollinger AT, Božović I (2016) Two-dimensional superconductivity in the cuprates revealed by atomic-layer-by-layer molecular beam epitaxy. *Supercond Sci Technol* 29:103001. <https://doi.org/10.1088/0953-2048/29/10/103001>
- Sen K, Marsik P, Das S, Perret E, de Andres Prada R, Alberca A, Biškup N, Varela M, Bernhard C (2017) Superconductivity and charge-carrier localization in ultrathin $\text{La}_{1.85}\text{Sr}_{0.15}\text{CuO}_4/\text{La}_2\text{CuO}_4$ bilayers. *Phys Rev B* 95:214506. <https://doi.org/10.1103/PhysRevB.95.214506>
- Alegria LD, Böttcher CGL, Saydjari AK, Pierce AT, Lee SH, Harvey SP, Vool U, Yacoby A (2021) High-energy quasiparticle injection into mesoscopic superconductors. *Nat Nanotechnol* 16:404–408. <https://doi.org/10.1038/s41565-020-00834-8>
- Katzer C, Stahl C, Michalowski P, Treiber S, Schmidl F, Seidel P, Albrecht J, Schütz G (2013) Gold nanocrystals in high-temperature superconducting films: creation of pinning patterns of choice. *New J Phys* 15:113029. <https://doi.org/10.1088/1367-2630/15/11/113029>
- Wang F, Lee DH (2011) The electron-pairing mechanism of iron-based superconductors. *Science* 332:200–204. <https://doi.org/10.1126/science.1200182>
- Ramallo MV, Vidal F (1999) Fluctuation specific heat in multilayered superconductors: bilayered Gaussian–Ginzburg–Landau scenario for the thermal fluctuations of Cooper pairs around T_c in $\text{YBa}_2\text{Cu}_3\text{O}_{7-\delta}$. *Phys Rev B* 59:4475–4485. <https://doi.org/10.1103/PhysRevB.59.4475>
- Hohenberg PC, Halperin BI (1977) Theory of dynamic critical phenomena. *Rev Mod Phys* 49:435–479. <https://doi.org/10.1103/RevModPhys.49.435>
- Kosterlitz JM, Thouless D (1973) Ordering, metastability and phase transitions in two-dimensional systems. *J Phys C* 6:1181–1203. <https://doi.org/10.1088/0022-3719/6/7/010>
- Halperin BI, Nelson DR (1979) Resistive transition in superconducting films. *J Low Temp Phys* 36:599–616. <https://doi.org/10.1007/BF00116988>
- Lawrence WE, Doniach S (1971) Theory of layer structure superconductors. In: Kanda E (ed) *Proceedings of twelfth international conference on low temperature physics*. Academic Press of Japan, Tokyo, pp 361–362
- Viña J, Campá JA, Carballeira C, Currás SR, Maignan A, Ramallo MV, Rasines I, Veira JA, Wagner P, Vidal F (2002) Universal behavior of the in-plane paraconductivity of cuprate superconductors in the short-wavelength fluctuation regime. *Phys Rev B* 65:212509. <https://doi.org/10.1103/PhysRevB.65.212509>
- Carballeira C, Mosqueira J, Ramallo MV, Veira JA, Vidal F (2001) Fluctuation-induced diamagnetism in bulk isotropic superconductors at high reduced temperatures. *J Phys Condens Matter* 13:9271–9279. <https://doi.org/10.1088/0953-8984/13/41/316>
- Rey RI, Ramos-Álvarez A, Mosqueira J, Ramallo MV, Vidal F (2013) Comment on “Diamagnetism and Cooper pairing above T_c in cuprates”. *Phys Rev B* 87:056501. <https://doi.org/10.1103/PhysRevB.87.056501>
- Tsuzuki T (1972) On the long-range order in superconducting intercalated layer compounds. *J Low Temp Phys* 9:525–538. <https://doi.org/10.1007/BF00655310>
- Quader KF, Abrahams E (1988) Superconducting fluctuations in specific heat in a magnetic field: dimensional crossover. *Phys Rev B* 38:11977–11980. <https://doi.org/10.1103/PhysRevB.38.11977>
- Thouless DJ (1960) Perturbation theory in statistical mechanics and the theory of superconductivity. *Ann Phys* 10:553–588. [https://doi.org/10.1016/0003-4916\(60\)90122-6](https://doi.org/10.1016/0003-4916(60)90122-6)
- Ferrell RA (1969) Fluctuations and the superconducting phase transition: critical specific heat and paraconductivity. *J Low Temp Phys* 1:241–271. <https://doi.org/10.1007/BF00628412>
- Ullah S, Dorsey AT (1991) Effect of fluctuations on the transport properties of type-II superconductors in a magnetic field. *Phys Rev B* 44:262–273. <https://doi.org/10.1103/PhysRevB.44.262>
- Puica I, Lang W (2003) Critical fluctuation conductivity in layered superconductors in a strong electric field. *Phys Rev B* 68:054517. <https://doi.org/10.1103/PhysRevB.68.054517>
- Vidal F, Carballeira C, Currás SR, Mosqueira J, Ramallo MV, Veira JA, Viña J (2002) On the consequences of the uncertainty principle on the superconducting fluctuations well inside the normal state. *Europhys Lett* 59:754–759. <https://doi.org/10.1209/epl/i2002-00190-3>
- Carballeira C, Mosqueira J, Revcolevschi A, Vidal F (2000) First observation for a cuprate superconductor of fluctuation-induced diamagnetism well inside the finite-magnetic-field regime. *Phys Rev Lett* 84:3157–3160. <https://doi.org/10.1103/PhysRevLett.84.3157>
- Mosqueira J, Ramallo MV, Currás SR, Torró C, Vidal F (2002) Fluctuation-induced diamagnetism above the superconducting transition in MgB_2 . *Phys Rev B* 65:174522. <https://doi.org/10.1103/PhysRevB.65.174522>
- Klemm RA (1990) Phenomenological model of the copper oxide superconductors. *Phys Rev B* 41:2073–2097. <https://doi.org/10.1103/PhysRevB.41.2073>
- Baraduc C, Buzdin A (1992) Fluctuations in layered superconductors: different inter-plane coupling and effect on the London penetration depth. *Phys Lett A* 171:408–414. [https://doi.org/10.1016/0375-9601\(92\)90666-A](https://doi.org/10.1016/0375-9601(92)90666-A)
- Vargunin A, Örd T (2014) Shrinking of the fluctuation region in a two-band superconductor. *Supercond Sci Technol* 27:085006–085014. <https://doi.org/10.1088/0953-2048/27/8/085006>
- Galteland PN, Subdø A (2016) Current loops, phase transitions, and the Higgs mechanism in Josephson-coupled multicomponent superconductors. *Phys Rev B* 94:054518. <https://doi.org/10.1103/PhysRevB.94.054518>
- Sellin K, Babaev E (2016) First-order phase transition and tricritical point in multiband $U(1)$ London superconductors. *Phys Rev B* 93:054524. <https://doi.org/10.1103/PhysRevB.93.054524>
- Stanev V, Tešanović Z (2010) Three-band superconductivity and the order parameter that breaks time-reversal symmetry. *Phys Rev B* 81:134522. <https://doi.org/10.1103/PhysRevB.81.134522>
- Chapman SJ, Du Q, Gunzburger MD (1995) On the Lawrence–Doniach and anisotropic Ginzburg–Landau models for layered superconductors. *SIAM J Appl Phys* 55:156–174. <https://doi.org/10.1137/S0036139993256837>

Publisher's Note Springer Nature remains neutral with regard to jurisdictional claims in published maps and institutional affiliations.